

RESEARCH ARTICLE

Performance analysis of unpowered lower limb exoskeleton during sit down and stand up

Yongfeng Wang^{1,2} , Guoru Zhao^{2,*} , Yanan Diao², Yu Feng¹ and Guanglin Li²

¹Hubei Key Laboratory of Intelligent Conveying Technology and Device, Hubei Polytechnic University, Huangshi 435003, China and ²CAS Key Laboratory of Human-Machine Intelligence-Synergy Systems, Shenzhen Institutes of Advanced Technology (SIAT), Chinese Academy of Sciences (CAS), Shenzhen, China

*Corresponding author. E-mail: gr.zhao@siat.ac.cn

Received: 22 March 2021; **Revised:** 30 June 2021; **Accepted:** 6 July 2021; **First published online:** 18 October 2021

Keywords: unpowered lower limb exoskeleton; stiffness of joints; contribution degree of muscles; metabolic cost.

ABSTRACT

Conventional unpowered lower limb exoskeleton paid little attention to the metabolic cost of body during sit down (SD)/stand up (SU). The SD motion model and the motion characteristics of lower extremity are analyzed; then, a novel unpowered lower limb exoskeleton is proposed, and the contribution degree of muscles and stiffness of joints are used for determining the location and stiffness of energy storage element. The metabolic cost of relevant muscles in joints of the left leg is obtained based on Opensim software. The results show that metabolic cost of the gracilis, rectus femoris (RF), and long head of the biceps femoris decreased about 13%, 9%, and 68%, respectively. The total metabolic cost of body decreased about 14% during SD. However, the metabolic cost of the gracilis, RF, and long/short head of the biceps femoris increased about 22%, 33%, 208%, and 46%, respectively. And the metabolic cost of sartorius reduces about 39%, the total metabolic cost of body increased about 25.6% during SU, under the exoskeleton conditions. The results of this study can provide a theoretical basis for the optimal design of unpowered lower limb exoskeleton.

1. Introduction

Stand up (SU) and sit down (SD) movements are essential parts of daily human activity, and vital for independence in persons with disability, which caused by nervous disorder, muscle damage, and other diseases [1]. SU is destabilizing in nature, as the body rapidly changes from a stable seated position to a position with a relatively small base of support and a higher center of mass, but the SD is the inverse of above process. The importance of SU and SD is particularly evident when the ability deteriorates and manifests itself; it decreases the mobility-related quality of life and increases the risk of falls in the elderly as well as in persons with disabilities.

In recent years, the application of wearable exoskeleton has become more prominent as to provide alternative solutions for care-needing older adults and disabled individuals support in their daily movements, such as SU, SD, ascending and descending staircases [2, 3]. Wu *et al.* [4] present a self-adaptive control strategy used on lower limb exoskeleton to help paraplegic patients to SU and SD, but its speeds are slower than joints of normal people. Chen *et al.* [5, 6] present a wearable exoskeleton suit (CUHK-EXO) to help paralyzed patients regain the ability to walk, SU and SD. Safety tests for long-term wearing of CUHK-EXO will also be conducted in the future, including any adverse effect in the hip, groin, penis, back, wrist, glutei, and scapula of the wearers. Jatsun *et al.* [7] study on a lower limb exoskeleton performing standing up motion from a chair, and present a modified Jacobian transpose controller which allowed to implement the proposed combined control strategy. Karen Junius *et al.* [8] present an exoskeleton to assist the wearer during sit to stand activities, which driven by compliant mechanically

adjustable compliance and controllable equilibrium position actuator. In addition, the exoskeleton consists of six active flexion/extension joints. Kamali *et al.* [9] present a novel control approach for a knee exoskeleton to assist individuals with lower extremity weakness during sit-to-stand motion. It consists of a trajectory generator and an impedance controller; the misalignment errors reduce the effectiveness of the exoskeleton controller.

Above exoskeletons use many electric motors to help patients to SU or SD; it consumes large amounts of electric energy, and not able to work for long hours. Moreover, the complexity of control system of exoskeletons is added, because of the influence of controllers, sensor and electric source, and so on.

The power sources of the unpowered lower limb exoskeletons are gait energy, which includes the kinetic energy and gravitational potential energy of body. The energy storage element (spring, elastic strap, torsional spring, pneumatic muscle, etc.) is used to store gait energy, and the clutches change the work pattern of energy storage element at the right time. One of the earliest records of an unpowered exoskeleton to assist human walking was found in a patent; it has two bowsprings that spanned the length of the leg [10]. Collins *et al.* [11] designed a lightweight exoskeleton that provides some of the functions of the calf muscles and tendons during walking; it reduces the metabolic cost of walking about $7.2 \pm 2.6\%$ for healthy human users under natural gait conditions. Cherelle *et al.* [12] developed a minimally actuated transtibial prosthesis; it consists of three bodies pivoting around a common axis (the ankle) and uses a two-spring system to harvest energy throughout the stance phase, and the elastic potential energy of springs is released at toe-off. Hirai *et al.* [13] developed a passive ankle-foot orthosis; it uses a pneumatic element to provide a restraining force that can lock the ankle in a neutral position. Walsh *et al.* [14] presented a quasi-passive exoskeletal for load carrying that achieves an improved walking metabolic performance as compared to a standard loaded backpack; it transfers on average 80% of the load to the ground during the single support phase of walking. Scott and Marc [15] presented a passive ankle exoskeleton; it used a pneumatic artificial muscle (PAM) as a non-linear elastic element to store and release energy during walking. Dijk *et al.* [16] developed a passive lower limb exoskeleton that used artificial tendons to minimize the joint work during walking; it reduces human energy expenditure obviously. Lee *et al.* [17] presented an entirely soft and passive knee extension assist wear (X-tights); it is developed by an optimized tendon routing method using elastic bands inspired by the anatomical design of human knee extensor for effective force transfer across the lower body. Panizzolo *et al.* [18] proposed a passive wearable assistive device (Exoband); it applies a torque to the hip flexion, thus reducing the net metabolic power of wearers. Rome *et al.* [19] found that use of rubber bands in parallel with the hip joint can reduce the metabolic costs of carrying loads during walking. Haufe *et al.* [20] find that a spring attached anteriorly across the hip appears to store and return proportions of the elastic energy. As energy is returned, the spring assists hip flexion, while muscle activity related to ankle plantarflexion around push-off increases. Zhang [21] presented a passive lower limb exoskeleton suit; it utilizes the passive dynamics of level walking to convert mechanical energy otherwise dissipated during the gait cycle into elastic potential energy, and the mechanical work potential was increased when the energy was returned to assist the leg during a different period of the gait cycle. Rezvan *et al.* [22] designed an unpowered exoskeleton with a bent-leaf-spring (BLS); it reduces the metabolic cost of running by $8.0 \pm 1.5\%$ as compared with no-exoskeleton case. In addition, considering the exoskeleton mass in metabolic cost normalization, the average metabolic cost reduction is $10.2 \pm 1.5\%$. Ronnapeet *et al.* [23] developed an exoskeleton prototype using a crossing four-bar mechanism as a knee joint with an embedded torsion spring. Its total mass is 1070 g, compared with 490 g for the original knee brace, and it decreases muscle activity of rectus femoris (RF). Matthew *et al.* [24] presented a novel unpowered ankle exoskeleton that is low profile, lightweight, quiet, low cost to manufacture, and intrinsically adapts to different walking speeds. It does not restrict non-sagittal joint motion and blends the torque assistance of the prior exoskeleton with the form-factor benefits of clothing. Leclair *et al.* [25] presented a lightweight unpowered ankle exoskeleton with PAM. The PAM were installed on the shank upright component; it harvests energy through the stance phase and releases the accumulated energy at push-off. Copilusi *et al.* [26] presented a low-cost exoskeleton with fairly simple construction, lightweight, easy to wear and to adapt to human legs. It used a cam-mechanism implementation at the ankle joint level using a low-cost

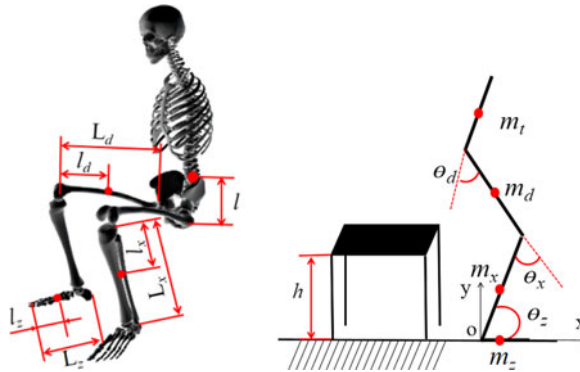


Figure 1. Sit down (SD) model of lower extremity.

biped mechanism. Ji *et al.* [27] developed a novel unpowered energy-stored exoskeleton (ES-EXO) for spinal cord injured patients. It provides specific walking assistance for SCI patients according to the parameters of energy-stored elements. The energy is stored by lumbar muscles contraction in stance phase and released in swing phase.

The stiffness of elastic elements for those unpowered lower extremity exoskeletons is fixed, but the stiffness of muscle is variable in the different activities of the human body, so elastic elements are inconvenient for the utilization gait energy, which weaken the assist effect of exoskeleton. Besides, most previous studies have paid little attention to the metabolic cost of body during SD/SU, ascending/descending staircases, and so on; it is unfavorable for evaluation and application of exoskeletons. The utilization mechanism of gait energy is described in detail in this paper, and the design principles of elastic energy storage element are determined, which contain the work mode, location, and stiffness. Then, a novel, modular, light mass unpowered lower extremity exoskeleton is presented; the metabolic cost of body during SD/SU is analyzed, under the exoskeleton conditions. This exoskeleton helps patients with abnormal gait to convenient, low cost, and stable walking.

The paper's structure is arranged as follows. Firstly, the SD of human model is established by Lagrange method, and bionics structure design of unpowered lower extremity exoskeleton is proposed in Section 2. It consists of elastic energy storage elements, clutch devices, waistband, kneepad, shoes, and so on. The forces of muscles, stiffness of joints, and contribution degree of muscles involve in SU and SD are analyzed in Section 3. Then the exoskeleton-muscular system is analyzed by the Opensim software system, and the metabolic cost of relevant muscles of lower extremity is obtained in Section 4, under different stiffness of energy storage components. Lastly, Section 5 summarizes the full paper.

2. Materials and methods

2.1. Dynamics analysis of lower extremity during SD

Motion analysis is a well-established tool for the quantitative assessment of activity ability of body; it includes the kinematics and kinetics analysis of body and provides functional diagnosis, assessment for treatment planning, and monitoring of disease progress for the person. Using vector analysis method, the inverse and forward kinematics solution of body are solved, and the motion characteristics of lower extremity is analyzed by Lagrange method in this paper. Compared to other methods, the Lagrange method has many remarkable advantages such as simple calculation process, take no account of friction loss and interacting forces in system. The lower extremity is regard as multibody dynamic model which consist of trunk, hip, knee, ankle and foot, as shown in Fig. 1. The mass of trunk, thigh, shank, and foot is m_t , m_d , m_x , and m_z ; the length of thigh, shank, and foot is l_d , l_x , l_z ; the distance between mass center and joints for trunk, thigh, shank, and foot is l , l_d , l_x , l_z ; the joint angle of hip, knee, and ankle is θ_d ; θ_x ; θ_z ; respectively.

According to the SD model of lower extremity, the mass center coordinates of foot are

$$h_{zx} = l_z, h_{zy} = 0, \tag{1}$$

the mass center coordinates of shank are

$$h_{xx} = (L_x - l_x) \cos \theta_z; h_{xy} = (L_x - l_x) \sin \theta_z \tag{2}$$

the mass center coordinates of thigh are

$$\begin{cases} h_{dx} = L_x \sin \theta_z - l_d \cos (180 - \theta_z - \theta_x) \\ h_{dy} = L_x \cos \theta_z + l_d \sin (180 - \theta_z - \theta_x) \end{cases} \tag{3}$$

the mass center coordinates of trunk are

$$\begin{cases} h_{tx} = L_x \sin \theta_z - L_d \cos (180 - \theta_z - \theta_x) + l \cos (\theta_x + \theta_z - \theta_d) \\ h_{ty} = L_x \cos \theta_z + L_d \sin (180 - \theta_z - \theta_x) + l \sin (\theta_x + \theta_z - \theta_d) \end{cases} \tag{4}$$

The velocity of mass center of trunk, thigh, and shank is obtained by taking the derivative of Formulas (2), (3), and (4), respectively. Then the total kinetic energy of single leg is obtained.

$$\begin{aligned} T &= \frac{1}{2} m_x v_x^2 + \frac{1}{2} J_{Cx} \dot{\theta}_z^2 + \frac{1}{2} m_d v_d^2 + \frac{1}{2} J_{Cd} \dot{\theta}_x^2 + \frac{1}{2} m_t v_t^2 + \frac{1}{2} J_{Ct} \dot{\theta}_d^2 \\ &= \frac{1}{2} m_x [(L_x - l_x) \dot{\theta}_z]^2 + \frac{1}{2} J_{Cx} \dot{\theta}_z^2 \\ &\quad + \frac{1}{2} m_d [L_x^2 + l_d^2 + 2L_x l_d \sin (\theta_z - \hat{\theta}) \dot{\theta}_z^2 + l_d^2 \dot{\theta}_x^2] + \frac{1}{2} J_{Cd} \dot{\theta}_x^2 \\ &\quad + \frac{1}{2} m_t [L_x^2 + L_d^2 + l^2 + 2L_x L_d \sin (\theta_z - \hat{\theta})] \dot{\theta}_z^2 \dot{\theta}_d^2 \\ &\quad - m_t [L_x l \sin (\theta_z + \bar{\theta}) + L_d l \cos (\hat{\theta} + \bar{\theta})] \dot{\theta}_z^2 \dot{\theta}_d^2 \\ &\quad + \frac{1}{2} m_t [L_d^2 + l^2 - 2L_d l \cos (\hat{\theta} + \bar{\theta})] \dot{\theta}_x^2 l^2 \dot{\theta}_d^2 + \frac{1}{2} J_{Ct} \dot{\theta}_d^2 \end{aligned} \tag{5}$$

where $\hat{\theta} = 180 - \theta_z - \theta_x, \bar{\theta} = \theta_x + \theta_z - \theta_d$

The total potential energy of single leg is P

$$\begin{aligned} P &= m_x g (L_x - l_x) \sin \theta_z + m_d g (L_x \cos \theta_z + l_d \sin (180 - \theta_z - \theta_x)) \\ &\quad + m_t g (L_x \cos \theta_z + L_d \sin (180 - \theta_z - \theta_x) + l \sin (\theta_x + \theta_z - \theta_d)) \end{aligned} \tag{6}$$

Lagrange equation is defined as the difference between kinetic energy (T) and potential energy (P), as Formulas (7) and (8):

$$L = T - P \tag{7}$$

$$M_j = \frac{d}{dt} \frac{\partial L}{\partial \dot{\theta}_j} - \frac{\partial L}{\partial \theta_j} \tag{8}$$

where $\theta_j, \dot{\theta}_j$ are the generalized angle and generalized velocity of hip, knee, and ankle, respectively.

$$p_i = M_i \dot{\theta}_j, \tag{9}$$

The joint power of body is described as working ability of joints; according to Eq. (9), the joint powers of lower extremity are obtained, respectively.

The motion capture system (Vicon) with AMTI force plates is considered the gold standard for human movement analysis in the field of biomechanics. The Vicon system used consists of six high resolution cameras that collect the infrared light reflected by retro-reflective markers in our laboratory, two AMTI force plates with a sampling frequency of 1000 Hz, as shown in Fig. 2.

Table I. The motion parameters of human [29]

Parameters	Values	Unit
Body height H	180	cm
Length of thigh L_d	40.7	cm
Length of shank L_x	39.8	cm
Length of foot L_z	25.6	cm
Body weight M	71.2	kg
Weight of trunk m_t	33.5	kg
Weight of thigh m_d	9.3014	kg
Weight of shank m_x	3.7075	kg
Weight of foot m_z	1.25	kg
Moment of inertia of trunk J_{Cr}	3081	kg • cm ²
Moment of inertia of thigh J_{Cd}	1412	kg • cm ²
Moment of inertia of thigh J_{Cx}	511	kg • cm ²
Distance between mass center and joint for trunk l	12	cm
Distance between mass center and joint for thigh l_d	17	cm
Distance between mass center and joint for shank l_x	18.67	cm
Distance between mass center and joint for foot l_z	10	cm

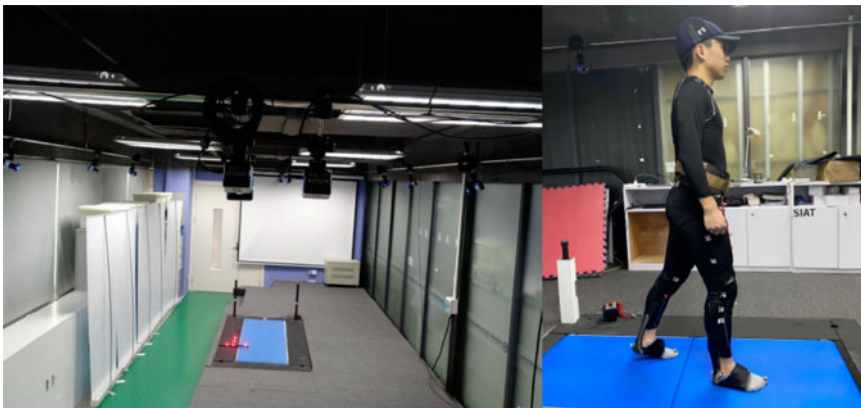


Figure 2. Vicon motion capture system.

The motion capture procedure is as follows: (1) a subject that is about 1.80 m and 71.2 kg, the motion parameters of human as shown in Table I. (2) the view parameters of high-speed camera are adjusted in biomechanics laboratory, make sure that the body in visual range of cameras and the coordinate calibration of cameras is set. (3) the body model with 31 markers is established in Opensim musculoskeletal system (gait2354-simbody), and the markers are pasted on the subjects at appropriate locations. (4) the motion data of human are dynamic and static collected by Vicon system, and they are patched and corrected; the angles of joints of lower extremity were acquired, as shown in Fig. 3.

During the normal gait, the angles of joint of lower extremity have obvious periodicity, and the originality datum needs further processing because of the tremble of limbs and trunk. So the datum of markers was analyzed by Fourier transform algorithm, which has many remarkable advantages such as simple calculation process, high efficiency, fast speed, and high fidelity [28]. The Fourier series equation can be described as follows:

$$f(t) = a_0 + \sum_{k=1}^m (a_k \cos \theta(k\omega t) + b_k \sin \theta(k\omega t)) \tag{10}$$

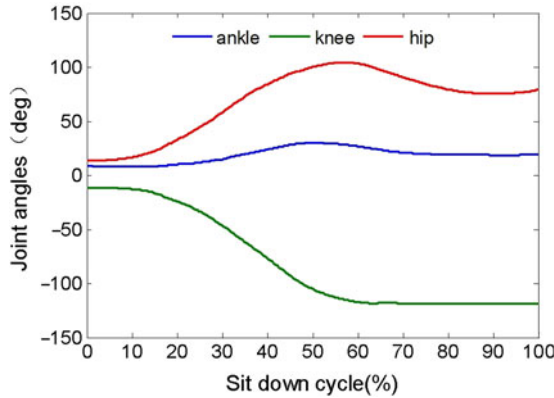


Figure 3. The angle of joints during SD.

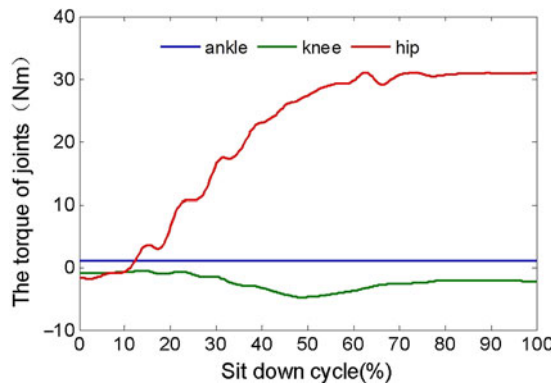


Figure 4. The torque of joints (left leg).

where a_0, a_k, b_k is the uncertainty coefficient of Fourier function, respectively; t is the time constant, m is the Fourier series coefficients, $m \leq \frac{n}{2}$. The Fourier series equation can be expressed as matrix form formulas (11).

$$AX = Y \tag{11}$$

$$X = [a_0, a_1, b_1, a_2, b_2 \dots a_n, b_n]$$

$$Y = [f(t_1), f(t_2) \dots f(t_n)]$$

$$X = (A^T A)^{-1} A^T Y$$

$$A = \begin{bmatrix} 1 & \cos(\omega t_1) & \sin(\omega t_1) & \cos(2\omega t_1) & \dots & \sin(m\omega t_1) & \cos(m\omega t_1) \\ 1 & \cos(\omega t_2) & \sin(\omega t_2) & \cos(2\omega t_2) & \dots & \sin(m\omega t_2) & \cos(m\omega t_2) \\ \vdots & \vdots & \vdots & \vdots & \ddots & \vdots & \vdots \\ 1 & \cos(\omega t_n) & \sin(\omega t_n) & \cos(\omega t_n) & \dots & \sin(m\omega t_n) & \cos(m\omega t_n) \end{bmatrix}$$

The uncertainty coefficients of Fourier function are an infinite series whose terms are constants multiplied by sine and cosine functions. It was calculated by least-squares method, and the accuracy was tested by means of residual and residual sum of squares. Then combine with formulas (5), (6), (9), (10) and motion parameters of human (Table I), the velocity, acceleration, torque, power of joints, and the

Table II. Uncertainty coefficient of Fourier function

Joints	a_0	a_1	a_2	a_3	a_4	a_5	a_6	a_7	a_8
Ankle	17.94	8.28	1.81	1.12	-0.41	0.39	-0.29	0.15	-0.19
Knee	-78.5	-56.3	15.96	2.06	-4.79	2.41	0.47	-1.07	-0.37
Hip	868.7	-403	-1239	-910.8	209.8	-450.1	120.2	28.64	11.56

Table III. Uncertainty coefficient of Fourier function

Joints	b_1	b_2	b_3	b_4	b_5	b_6	b_7	b_8	w
Ankle	2.54	-3.56	-0.2	-0.48	0.003	0.11	-0.15	0.14	2.06
Knee	-8.38	-2.49	8.5	-2.28	-2.43	1.92	-0.26	-0.37	1.92
Hip	-1501	761.7	730.1	-781.8	81.64	162.3	-56.43	-0.5788	1.216

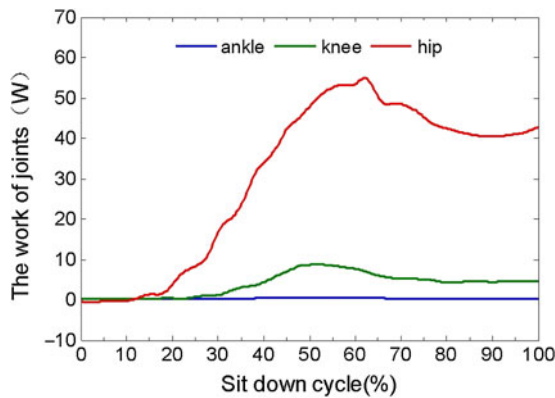


Figure 5. The work of joints (left leg).

coefficients of Fourier function of the joint angles were obtained, as shown in Figs. 4 and 5 and Tables II and III.

2.2. Structural design of unpowered lower extremity exoskeleton

2.2.1. Design principles of elastic energy storage element

Modular design is basically to decompose complex systems into simple modules in order to more efficiently organize complex designs and processes. Its advantages include design flexibility, augmentation, cost reduction, and so on [30]. So the unpowered lower limb exoskeleton is proposed in this paper, as shown in Fig. 6. It has simple structure, convenient wearing, lightweight, and adapt to different gait, and helps the patient to walk.

This exoskeleton consists of elastic energy storage elements, clutch devices, waistband, kneepad, shoe, and so on. Wherein, the elastic energy storage elements are natural rubber latex band, which has good flexibility, dry cleaning, no shrinkage, chlorine resistance, light fastness, and sweat resistance. And the waistband is Spandex; it has had an impact on fashion high and low, casual and formal, outer and under.

Human power is an attractive energy source; it contains kinetic energy, potential energy, and muscles works. Wherein the muscle converts food into positive mechanical work with peak efficiencies of approximately 25%, and about 30% positive mechanical of muscle for the body move forward.

There are multiple muscles in the ankle, such as the peroneus longus and peroneus brevis; they allow the ankle to bend downward and outward. The gastrocnemius and soleus are connected to the calcaneus

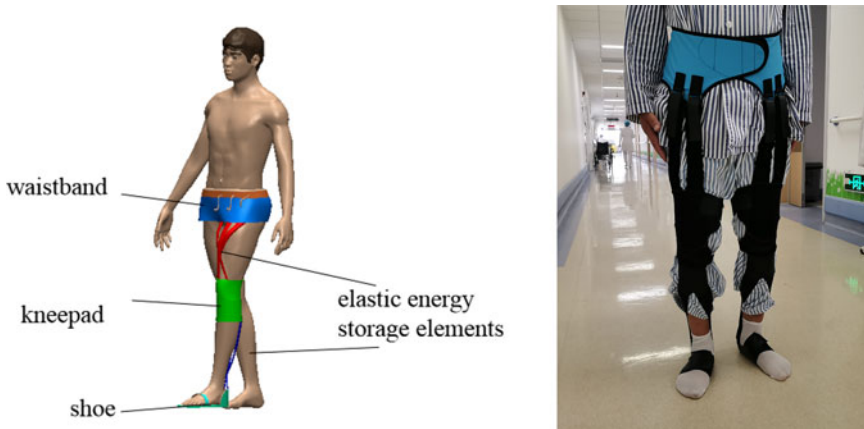


Figure 6. Structure of unpowered lower limb exoskeleton.

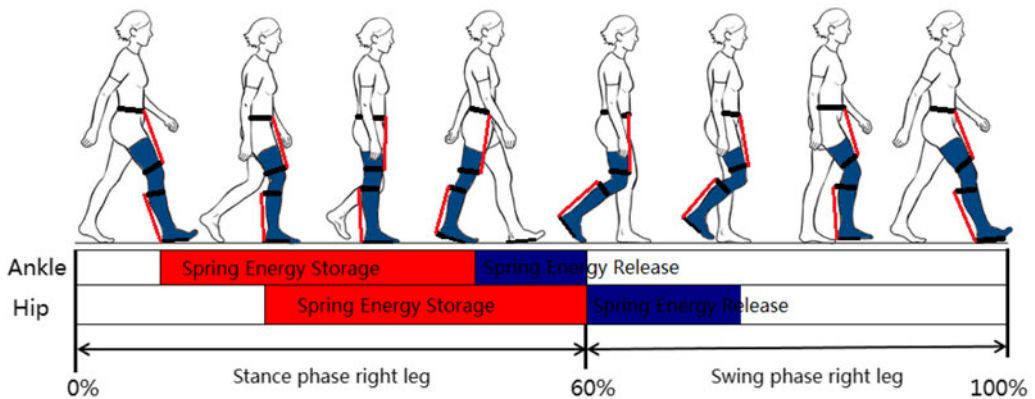


Figure 7. Energy storage and release of joints.

via the Achilles tendon; they enable the ankle to bend downward and upward. The posterior tibialis enables the foot to turn inward, but the anterior tibialis enables the ankle and foot to turn upward.

During the loading response and midterm of stance phase, the anterior tibial, gastrocnemius, and soleus are to take eccentric contraction; they maintain constant tension in the muscle as the muscle changes length, and to store the metabolic energy, which is similar to elastic energy storage elements. During late term of stance phase, they are taking concentric contraction, in which the muscles shorten due to the sliding filament mechanism, and metabolic energy was released, then they offer positive joint powers to propel the limb and body move upward and forward, the maximum of joint powers can approach to 3.6 W/kg [21], as shown in Fig. 7.

The dorsiflexion and flexion of ankle are the major motion during walking; the elastic energy storage element was installed on the front side of the shank reflects on the motion of toe, then it was installed on the both sides of the shank restrictions on the performance of exoskeleton, so the back side of the shank is an ideal location to install elastic energy storage element. The mechanical energy is converted into elastic potential energy that stored in the elastic energy storage element, during the loading response and midterm of stance phase, and it is released during heel off.

Moreover, the hip muscles include pelvic and groin muscles, such as RF, semimembranosus, tensor fasciae latae, and sartorius; they are important for stabilizing the body and for moving the legs. The hip has complicated structure; the elastic energy storage element is difficult to install on the back and both side of the hip, so the front side of the thigh is an ideal location to install elastic energy storage element. During the loading response and midterm of stance phase, the mechanical energy is converted

into elastic potential energy that stored in the elastic energy storage element, and it is released during toe off during the loading response and midterm of stance phase.

Taken together design principles of elastic energy storage element, the mechanical energy of limb is converted into the elastic potential energy of element during negative joint work, and the elastic potential energy of the element is released during positive joint work. Wherein, the positive joint work occurs when the muscles perform a concentric contraction while negative joint work occurs when the muscles elongate or stretch during an eccentric contraction. And the concentric contractions are the primary contributors that generate the work performed by the joint to increase the limb segment mechanical energy while eccentric contractions result in mechanical energy absorption as work is performed on the adjacent limb segments by an external force such as gravity. So the metabolic cost is associated with performing negative joint work or eccentric muscle contractions, and the cost is lower than that of positive joint work or concentric muscle contraction.

Gait energy contains the kinetic energy and gravitational potential energy of limbs; it is converted into elastic potential energy by the energy storage element, which is an important part in the unpowered exoskeletons. The energy storage element has several forms, such as helical spring [11, 21], BLS [22], pneumatic muscle [25], torsion springs [27], memory alloy [31], and rubber [32, 33].

For the energy storage element with helical spring, the direction of output force is in accord with the axis of helical spring; it has lightweight, without damping, high reset performance, and connects to the two adjacent limbs. However, the helical spring needs bigger space because of the stretch/shrink of helical spring, and the spring is easy to shake during tension procedure.

Torsion springs are helical springs that exert a torque or rotary force. The ends of torsion spring is attached to the rotational center of joint, and the torsion spring tries to push them back to their original position when limbs moment, but it limits the motion performance of joints.

Energy storage element contains shape memory alloy (SMA), which has high power density and can be restored to their original shape by heating after every use, and it only has passive elastic and damping components for shock energy absorption. Moreover, energy storage element uses the PAM as a linear actuator; it has significant longitudinal forces, non-linear tensile, and stiffness behavior. But the propagation velocity of PAM is slow, which compared to biological muscles.

The elastic material includes thermoplastic elastomer (TPE), thermoplastic polyurethanes (TPU), rubber, latex, and so on. The TPE and TPU have high resilience, high strength, small deformation, and oil resistance. And the rubber and latex have high elasticity, heat resistance, wear resistance, flexibility, and elasticity. They are the optimal choice for energy storage element.

Combined with the torques and angles of joints in SD and SU, the stiffness of hip, knee, and ankle is obtained, as shown in Fig. 8. The RF, gracilis, and sartorius act on the hip during SD, and the flexion angle and torque of hip reach maximum 104° , 31 Nm/kg , respectively. The extension angle and torque of hip gradually reduce to 10° , -2 Nm/kg , according to linear regression analysis for the datum of torque and angle, then the stiffness of hip is 0.348 Nm/kg/deg . The gracilis, sartorius, and biceps femoris act on the knee during SD, and the flexion angle and torque of knee reach maximum 110° , 5.5 Nm/kg , respectively, the extension angle and torque of knee gradually reduce to 5° , -0.5 Nm/kg , respectively, and then the stiffness of knee is 0.047 Nm/kg/deg . Meanwhile, the torque of ankle is very small during SD and SU, the extension angle of ankle reaches maximum 32° , the torque of ankle ranged between $0.95 \sim 1.01 \text{ Nm/kg}$, and the stiffness of ankle is 0.002 Nm/kg/deg .

2.2.2. Structure and work mode of clutch device

The gait energy in energy storage element is stored and released by the clutch device, and this device has the advantages of small volume, good flexibility, low cost, and high efficiency. The clutch device is composed of elastic energy storage elements, support plate, swing component, and so on. The middle of elastic energy storage element has many barbs, the lower part of support plate has a baffle, and the swing component contains micromotor, wireropes, gear, gear belts, and pawl. The pawl rotates around the pivot point that fixed on support plate, as shown in Fig. 9.

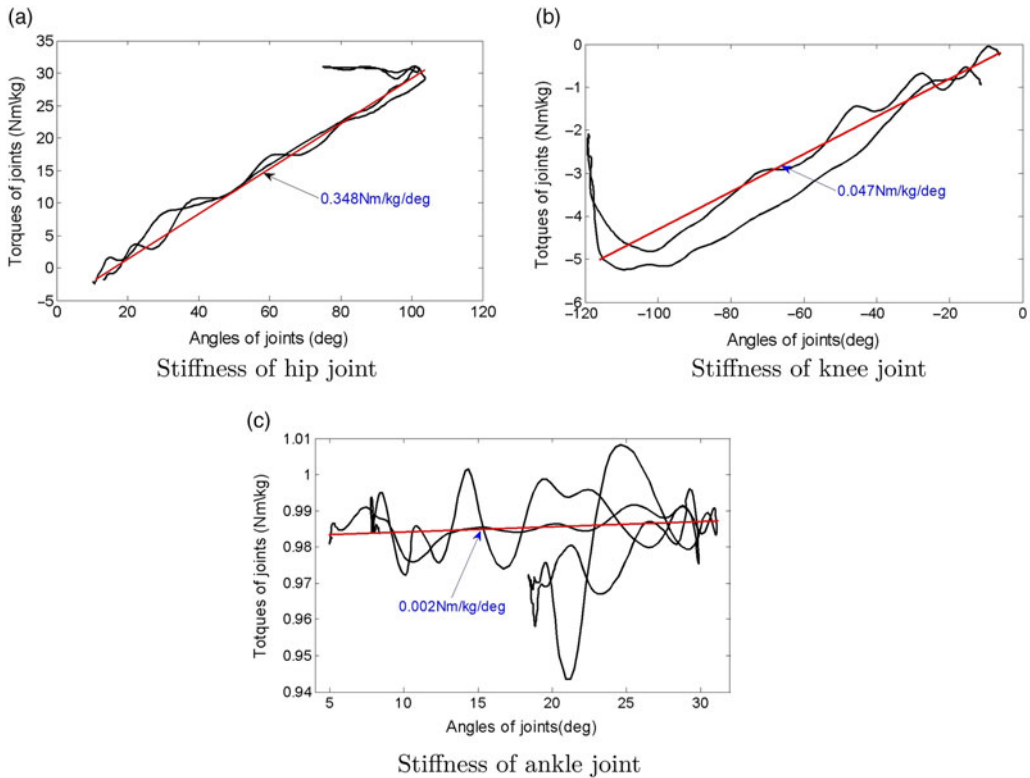


Figure 8. Stiffness of joints (left leg).

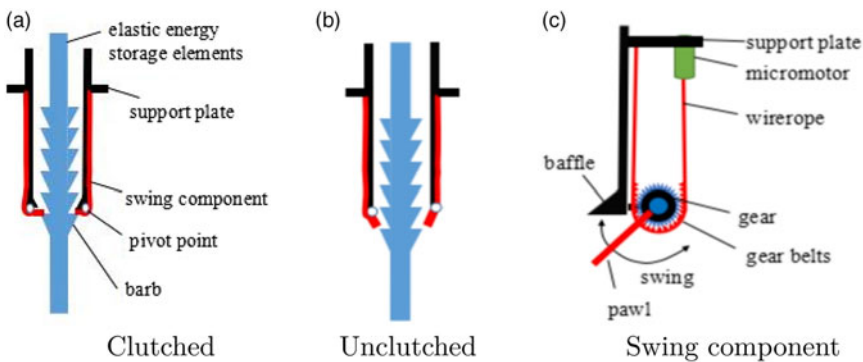


Figure 9. Structure of clutch device.

Take the clutch device of hip for example, the elastic energy storage elements were stretched and the gait energy is stored during the late term of stance phase, then the micromotor drive wireropes and gear belts move to baffle, the pawl engage with the barbs to restrict the elastic energy storage elements draw back. The elastic energy storage elements can not provide any forces to the hip joint and it not restrict the motion of thigh; during the early term of swing phase, the micromotor drive wireropes and gear belts move away to baffle when heel off state, the pawl disengage with the baffle, elastic energy storage element is shrunk, so the elastic potential energy is released to pull the thigh swing.

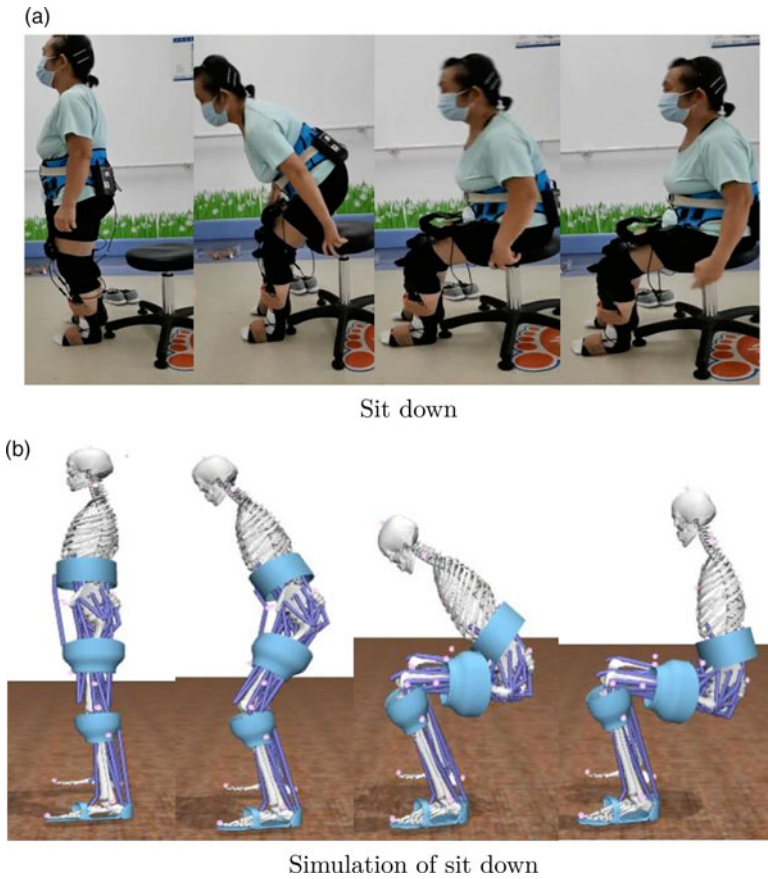


Figure 10. Sit down process.

2.3. Motion characteristics of lower limbs during SD and SU

2.3.1. SD process

SD and SU movements are essential parts of daily human activity. SD is a prerequisite for most human activities, such as walking, running, and climbing stairs. Four phases have been recognized as crucial for the description and analysis of the SD movement: (1) The body's center of gravity is located in the front third sacral vertebra about 7 cm, then the gluteus maximus, quadriceps femoris, triceps surae, and erector spinae work together to keep human body in a stable state; (2) The head, arms, and trunk rotate forward around the pelvis, the hip and knee joint in flexion and the ankle joint in dorsiflexion, and the buttocks start contacting the chair. Moreover, the chair has suffered an impact force by body; it hinders the body's center of gravity move down toward; (3) the muscles in buttocks and waist helps the body move back toward, the body's center of gravity at the center of the seat of the chair; (4) the position of foot and posture of body are adjusted slightly, the person sits in optimal state, as shown in Fig. 10.

2.3.2. Contribution degree of muscles of joints

The skeletal muscles in the lower limb of body work together on the joints, and they help body walk in various complicated environments. When some skeletal muscles of joints were damaged, the abnormal gait of body was happened, such as the ducks step which cause by the gluteus medius muscle weakness, the drags step which cause by quadriceps femoris muscle weakness, and the strides step which cause by ankle dorsal extensor muscle weakness.

Muscle synergy is defined as a combination of the limited number of muscle activities, which has been considered useful for controlling a large number of degrees of freedom in the musculoskeletal system. The contribution degree is used to evaluate the muscles participation during walk; the muscle forces of joints are obtained by gait analysis and musculoskeletal system (Opensim), and the normalization processing of datum is carried out. According to Formulas (12), the contribution degree of muscles for the hip and knee joint of left leg is shown in Fig. 11.

$$\eta = \frac{f_i}{f_1 + f_2 \cdots f_n} \tag{12}$$

where f_i is the force for the i th muscle in joint.

The force of sartorius, gracilis, and RF is about $[1.5\ 2.7] \times 10^4 N$, $[1.45\ 1.65] \times 10^4 N$, $[0\ 0.2] \times 10^4 N$, respectively. The contribution degree of sartorius and gracilis is about $[0.5\ 0.65]$, $[0.35\ 0.55]$, respectively. They are mainly acting on the hip flexion/extend during SD and SU. The force of sartorius, gracilis, the long head and short head of the biceps femoris is about $[1.7\ 2.8] \times 10^4 N$, $[1.5\ 1.6] \times 10^4 N$, $[0\ 1.5] \times 10^4 N$, $[1.5\ 5] \times 10^4 N$, respectively. And their contribution degree is about $[0.26\ 0.32]$, $[0.17\ 0.23]$, $[0\ 0.22]$, $[0.29\ 0.53]$, respectively. They help knee to flexion and extend. Besides, the sartorius and gracilis are involved in the motion of hip and knee during SD and SU.

3. Results

Energy cost is the energy contribution values from the macronutrients of fats, carbohydrates and proteins. Wherein, the resting energy cost is the minimal amount of energy required to support the body’s physiological functions; it is influenced by an individual’s amount of lean muscle mass, age, gender, and climate. During rest, various organs are responsible for consuming energy to support their functions. The resting energy cost is 1 met, and energy cost of sitting or writing is 2 met, running is about 3.3~38.7 met for normal people.

The metabolic cost of muscle contains activation heat, maintenance heat, shortening/lengthening heat, and mechanical work rate of the contractile element (CE); it was expressed as the sum of four terms [34].

$$\dot{E} = \dot{h}_A + \dot{h}_M + \dot{h}_{SL} + \dot{w}_{CE} = \dot{h}_{AM} + \dot{h}_{SL} + \dot{w}_{CE} \tag{13}$$

where \dot{h}_A is the activation heat rate, \dot{h}_M is the maintenance heat rate, \dot{h}_{SL} is the shortening/lengthening heat rate, \dot{w}_{CE} is the mechanical work rate of the CE. $\dot{h}_{AM} = \dot{h}_A + \dot{h}_M = 1.28 \times \%FT + 25$.

FT is the human fast twitch muscle fibers.

ST is the human slow twitch muscle fibers.

The shortening heat coefficients for ST and FT fibers are thus calculated as

$$\dot{a}_{S(ST)} = \frac{4 \times 25}{\tilde{V}_{CE(MAX-ST)}} \tag{14}$$

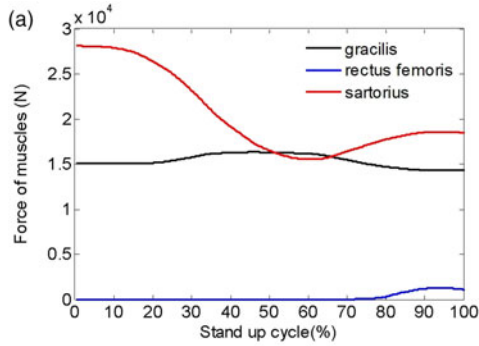
$$\dot{a}_{S(FT)} = \frac{4 \times 25}{\tilde{V}_{CE(MAX-FT)}} \tag{15}$$

where $\tilde{V}_{CE(MAX-ST)}$, $\tilde{V}_{CE(MAX-FT)}$ is defined by the Hill coefficients. The shortening heat rate is then given by

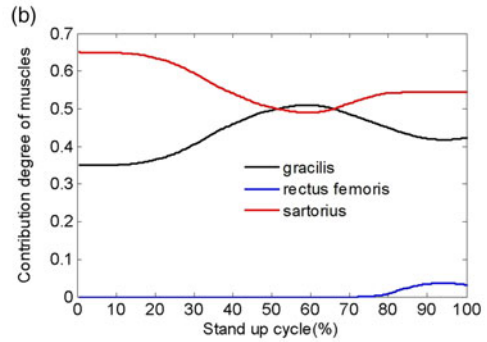
$$\dot{h}_{SL} = -a_{S(ST)} \tilde{V}_{CE}(1 - \%FT/100) - a_{S(FT)} \tilde{V}_{CE}(1 - \%FT/100) \tag{16}$$

The mass specific mechanical work rate is given by

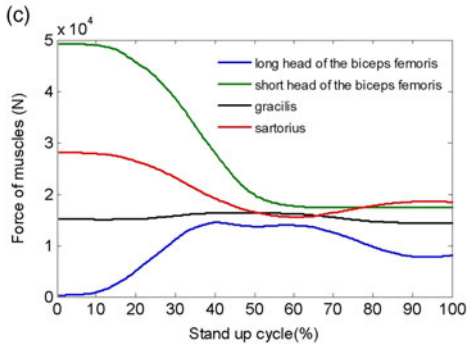
$$\dot{w}_{CE} = \frac{F_{CE} V_{CE}}{m} \tag{17}$$



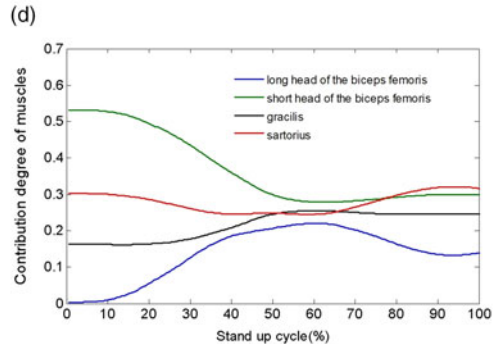
Metabolic cost of gracilis



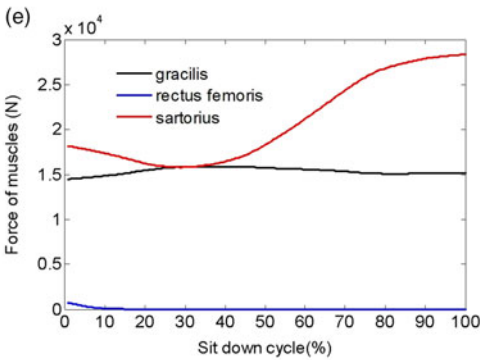
Metabolic cost of rectus femoris



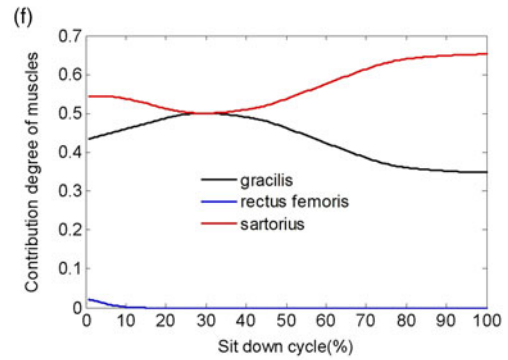
Metabolic cost of sartorius



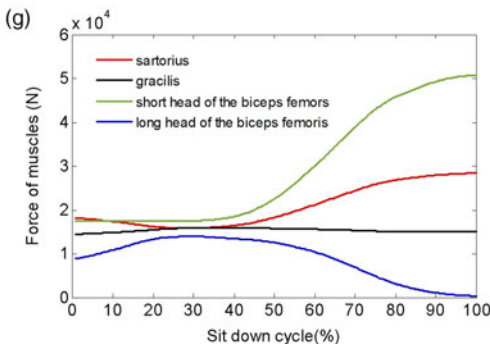
Metabolic cost of long head of the biceps femoris



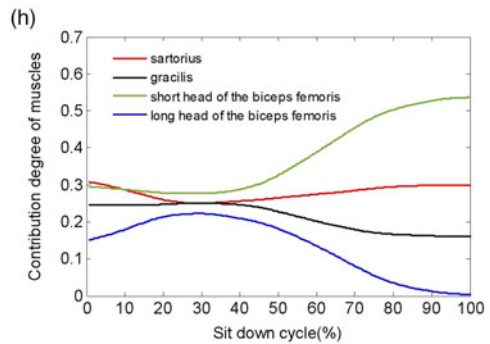
Metabolic cost of short head of the biceps femoris



Total metabolic cost



Metabolic cost of short head of the biceps femoris



Total metabolic cost

Figure 11. Metabolic cost for some muscles and body (left leg).

Table IV. Structure parameters of unpowered lower limb exoskeleton

Parameters	Values	Unit
Mass of thigh assisting device	0.8	kg
Mass of shank assisting device	0.7	kg
Length of energy storage element of hip	10	cm
Nominal diameter of energy storage element of hip	3.5	cm
Length of energy storage element of ankle	14	cm
Nominal diameter of energy storage element of ankle	2.4	cm
Length of pawl	3	cm
Diameter of gear of swing component	1.2	cm
Module of gear of swing component	0.1	cm

m is the mass of the muscle. Combined with Formulas (13)–(18), the metabolic cost of muscle is obtained from the following equation:

$$\begin{aligned}
 & \text{if } L_{CE} \leq L_{CE(OPT)}; \dot{E} = \dot{h}_{AM}A_{AM}S - (F_{CE}V_{CE})/m + W_{V1} \\
 & \text{if } \tilde{V}_{CE} \leq 0; W_{V1} = (-a_{S(ST)}\tilde{V}_{CE}(1 - \%FT/100) \\
 & \quad - a_{S(ST)}\tilde{V}_{CE}(1 - \%FT/100))A_S S \\
 & \text{if } \tilde{V}_{CE} > 0; W_{V1} = a_L\tilde{V}_{CE}AS \\
 & \text{if } L_{CE} > L_{CE(OPT)}; \dot{E} = (0.4 \times \dot{h}_{AM} + 0.6 \times \dot{h}_{AM}F_{ISO})A_{AM}S \\
 & \quad + (F_{CE}V_{CE})/m + W_{V2} \\
 & \text{if } \tilde{V}_{CE} \leq 0; \\
 & \quad W_{V2} = (-a_{S(ST)}\tilde{V}_{CE}(1 - \%FT/100) - a_{S(ST)}\tilde{V}_{CE}(1 - \%FT/100))F_{ISO}A_S S \\
 & \text{if } \tilde{V}_{CE} > 0; W_{V1} = a_L\tilde{V}_{CE}F_{ISO}AS
 \end{aligned} \tag{18}$$

where S is a scaling factor; under the anaerobic condition, the value of S is 1, but it is 1.5 under aerobic conditions; it is needed to account for the length and activation dependence \dot{h}_{AM} and \dot{h}_{SL} , factors for scaling \dot{h}_{AM} and \dot{h}_{SL} that depend on A .

$$\begin{aligned}
 A &= \begin{cases} STIM & \text{when } STIM > ACT \\ (STIM + ACT)/2 & \text{when } STIM \leq ACT \end{cases} \\
 A_{AM} &= A^{0.6}, A_S = A^{2.0}
 \end{aligned} \tag{19}$$

F_{CE} is the force of CE, V_{CE} is the velocity of CE. \tilde{V}_{CE} is the speed of CE, F_{ISO} is the force of isometric of muscle, $STIM$ is an idealized neurocontrol signal, ACT is muscle active state.

The musculoskeletal and metabolic cost models are used to estimate metabolic energy by Opensim software, and the steps for computing metabolic cost of musculoskeletal simulation in OpenSim are shown in Fig. 12. The scale model is scaled to match the anthropometry of subject; the inverse kinematics (IK) is solved to determine the joint angles that best reproduce the raw marker data obtained from Vicon system. The RRA is applied to make for the joint angles and translations of model, which more dynamically consistent with the measured ground reaction forces and moments. The CMC is used to generate a set of muscle excitations that produce a coordinated muscle-driven simulation of the subjects movement. According to the above data and the Umberger 2010 MuscleMetabolicsProbe, the structural parameters of energy storage elements are shown in Table IV. Wherein, the stiffness of energy storage elements for hip and ankle is $k_1=0.2, 0.4, 0.6, 0.8$ N/mm; $k_2=0.5, 0.6, 0.7, 0.8$ N/mm, respectively. So the metabolic cost of musculoskeletal model with exoskeleton was obtained, as shown in Fig. 13.

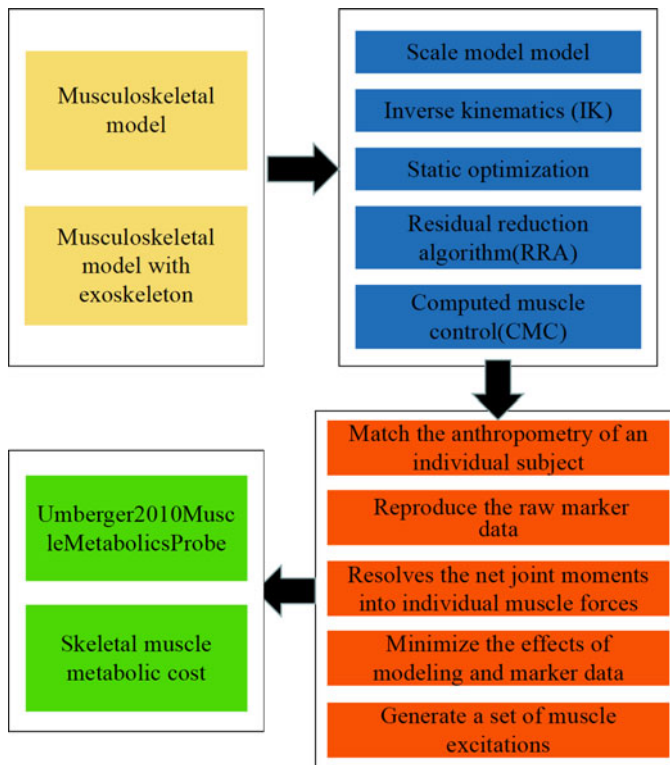


Figure 12. Steps for generating metabolic cost of musculoskeletal simulation in OpenSim.

In the early stage of SD, standing balance of body was broke, and the gracilis femoris and long head of the biceps femoris do negative work because of the eccentric contraction of muscles, and their energy cost steadily reduces about 0.7 J, 0 J; the RF, sartorius, and short head of the biceps femoris do positive work by the isokinetic contraction of muscles, and their energy cost steadily increases about 3.5 J, 2.1 J, and 3.9 J, respectively. In the middle stage of SD, gracilis and long head of the biceps femoris provide positive work to help the hip flex, their energy cost steadily increases about 1.5 J, 8.4 J. The RF, sartorius, and the short head of the biceps femoris do positive work, and their energy cost steadily reduces about 0.5 J, 0.5 J, 0.2 J. In the final stage of SD, gracilis, sartorius, and long head of the biceps femoris do negative work by gravity of body, the hip continues flex until the buttocks contact with the seat of the chair, then their energy cost steadily reduces about 0.5 J, 0.5 J; RF and sartorius do positive work to help the knee maintain flexion, and their energy cost steadily increases about 4 J, 1.6 J. Besides, the short head of the biceps femoris does small positive work, and its energy cost increases about 2.5 J. During the SU stage, the gracilis, RF, sartorius, and biceps femoris do positive work to help the hip and knee extending, and their energy cost steadily increases about 3.1 J, 1.5 J, 2 J, 2.2 J; but the RF does negative work, its energy cost reduces about 1.6 J.

Person SD under the exoskeleton conditions; the metabolic cost reduces about 13%, 9%, 68% for the gracilis, RF, and long head of the biceps femoris, but the metabolic cost of sartorius and the short head of the biceps femoris increases about 16%, 7%, and then the total metabolic cost reduces about 14%; during SU stage, the metabolic cost of the gracilis, RF, and long/short head of the biceps femoris increases about 22%, 33%, 208%, and 46%, but the metabolic cost of sartorius reduces about 39%; then the total metabolic cost increases about 25.6%, because of the elastic energy storage elements hinder the elongation of muscles. Moreover, the lower extremity exoskeletons can cause muscle activity happen much sooner.

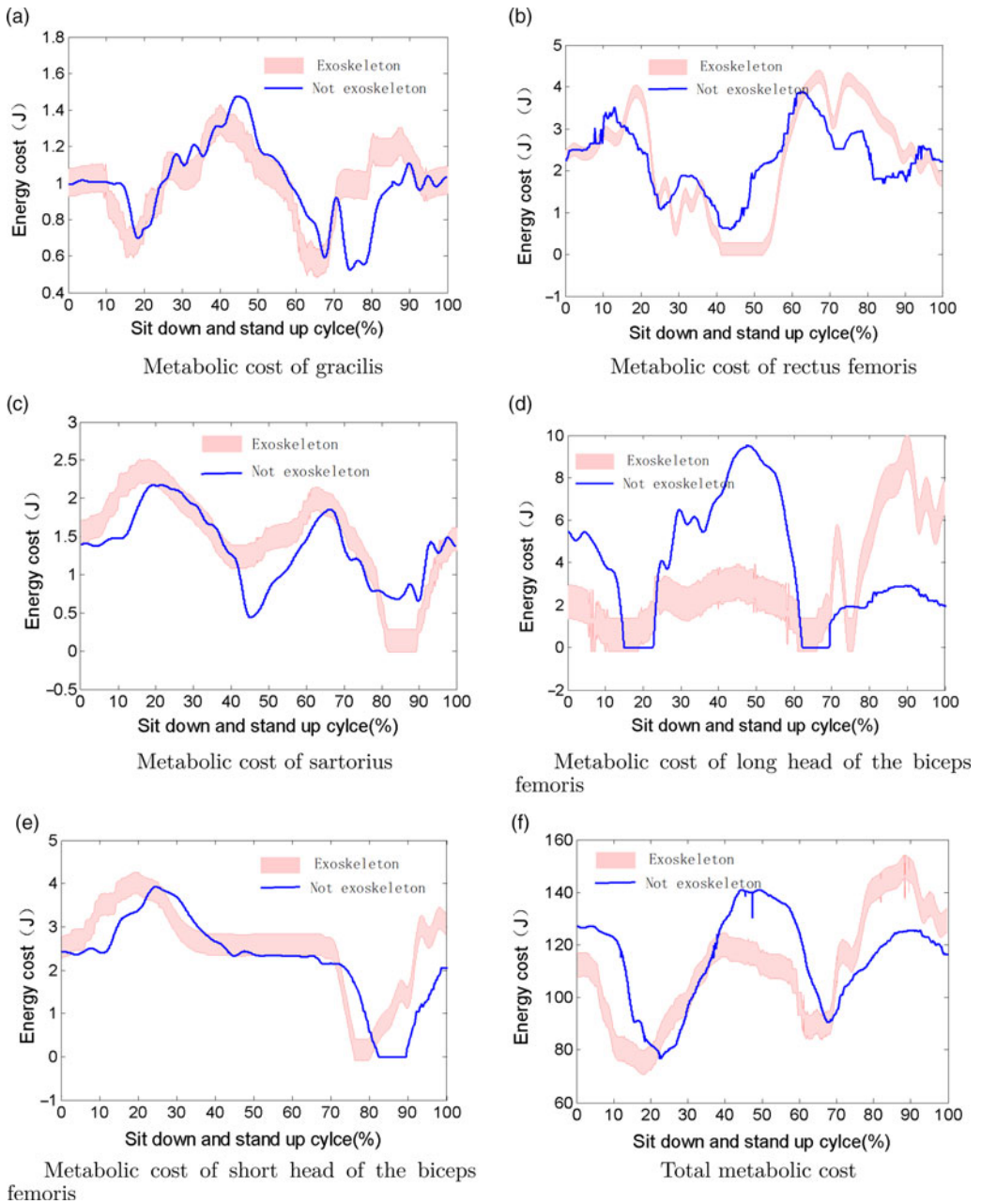


Figure 13. Metabolic cost for some muscles and body (left leg).

4. Conclusion

The aim of the present work was to design an unpowered lower limb exoskeleton which might be used by elderly people. It reduces the metabolic cost of body for normal daily living, and the mobility functionalities of lower extremity exoskeletons adapt to different kinds of occasions, such as straight walking on ground, bending down, walking up/downstairs, stepping over objects, and sit-to-stand transfers. Besides, the exoskeleton has many advantages such as comfortable, good fit, easy to put on/take off (don/doff), wearing without help, and lightweight.

The numerous numbers of researches and institutes make a profound study on the unpowered lower limb exoskeletons, but the gait energy is one of the key factors for the exoskeleton; it is composed of the swing and torso energy from sagittal and frontal dynamics (3LP dynamics), velocity redirection of center of mass (CoM), ground clearance, and weight support energy [35]. Moreover, the gait energy is closely related to the size, weight of body, the velocity of limbs, and trunk, so its utilization efficiency needs to be improved, which helps patients with abnormal gait to convenient, low cost, and stable walking.

The optimum design of structure and position of energy storage element base on the performance of muscle, which collects enough gait energy. For the helical spring, it needs bigger space and easy to shake during straining state. Torsion springs are attached to the rotational center of joint; it limits the motion performance of joints. The force transmissibility performance of SMA and PAM is slow compared to biological muscles. TPE and TPU have high resilience, high strength, and small deformation. In addition, the rubber and latex have high elasticity, heat resistance, wear resistance, flexibility, and elasticity. The mixture of them is the optimal choice for energy storage element.

The clutch device changes the work ways of energy storage element, it causes the gait energy is stored and released at appropriate time, which consider activation degree of muscle. And the muscles in limb take eccentric contraction to produce the mechanical energy of joints, which change into elastic potential energy of energy storage element. When the clutch device is unclutched, the elastic potential energy of energy storage element is released, then it offers positive joint powers to propel the limb and body move.

The paths of the forces for the energy storage element determine the quality and efficiency of energy storage element; bionic design of the paths of the forces for the energy storage element is based on transmission path of muscle. There are three main methods of description transmission path of muscle: lines enveloping, polygonal line with starting and ending points and curve path with obstacle [36]. Besides, the performance evaluation method for the unpowered lower extremity exoskeletons needs system optimization and adds some sensing elements to test the human condition and operating status of exoskeletons.

Acknowledgements. Yongfeng Wang helped in conceiving the study concept and design, acquiring the data, analyzing and interpreting the data, and drafting the manuscript. Feng Yu and Yanan Diao helped in acquiring the data, analyzing and interpreting the data, and drafting the manuscript. Guoru Zhao and Guanglin Li helped in conceiving the study concept and design, drafting and revising the manuscript, obtaining funding, and supervising the study. The authors would like to acknowledge Kai Zhen, Lili Liu, and Jing Yang for their help in collecting and analyzing the data of body, and operating of the Vicon equipment. All authors have read and agreed to the published version of the manuscript.

Funding. This study has been financed partially by the National Key R&D Program of China (2019YFB1311400/01, 2018YFC2001400/04), Shenzhen Science and Technology Development Fund (JCYJ20170818163505850), Shandong Key R&D Program (2019JZZY011112), the Innovation Talent Fund of Guangdong Tezhi Plan (2019TQ05Z735), High Level-Hospital Program, Health Commission of Guangdong Province (HKUSZH201901023), Guangdong-Hong Kong-Macao Joint Laboratory of Human-Machine Intelligence-Synergy Systems (2019B121205007), Hubei Key Laboratory of intelligent Conveying technology and device, Hubei Polytechnic University (2020XZ106, 19XJK16R), and the Key Project of Scientific Research Plan of Education Department of Hubei Province (No. D20204501).

Institutional Review Board Statement. Not applicable. Informed Consent Statement: Not applicable.

Conflicts of Interest. The authors declare that the research was conducted in the absence of any commercial or financial relationships that could be construed as a potential conflict of interest.

Supplementary Material. To view supplementary material for this article, please visit <https://doi.org/10.1017/S0263574721001077>.

References

- [1] G. E. Frykberg and C. K. Häger, "Movement analysis of sit-to-stand—research informing clinical practice," *Phys. Ther. Rev.* **20**(3), 156–167 (2015).
- [2] A. Norhafizan, R. A. R. Ghazilla, V. Kasi, Z. Taha and B. Hamid, "A review on lower-Limb exoskeleton system for sit to stand, ascending and descending staircase motion," *Appl. Mech. Mater.* **541**, 1150–1155 (2014).

- [3] S. Viteckova, P. Kutilek, G. de Boisboissel, R. Krupicka, A. Galajdova, J. Kauler, L. Lhotska and Z. Szabo, “Empowering lower limbs exoskeletons: State-of-the-art,” *Robotica* **36**(11), 1743–1756 (2018).
- [4] C. Wu, T. Zhang, Y. Liao, C. Wang, G. Wu and Wu, X. “Self-Adaptive Control Strategy for Exoskeleton to Help Paraplegic Patients Stand Up and Sit Down,” In: *Proceedings of the 35th Chinese Control Conference (CCC)* (2016) pp. 6189–6194.
- [5] B. Chen, C.-H. Zhong, X. Zhao, H. Ma, X. Guan, X. Li, F.-Y. Liang, J. C. Y. Cheng, L. Qin and S.-W. Law, “A wearable exoskeleton suit for motion assistance to paralysed patients,” *J. Orthop. Transl.* **11**, 7–18 (2017).
- [6] B. Chen, C.-H. Zhong, H. Ma, X. Guan, L.-Y. Qin, K.-M. Chan, S.-W. Law, L. Qin and W.-H. Liao, “Sit-to-stand and stand-to-sit assistance for paraplegic patients with CUHK-EXO exoskeleton,” *Robotica* **36**(4), 535–551 (2018).
- [7] S. Jatsun, S. Savin, A. Yatsun and I. Gaponov, “Study on a two-staged control of a lower-limb exoskeleton performing standing-up motion from a chair,” *Robot Intell. Technol. Appl.* **4**, 113–122 (2017).
- [8] K. Junius, B. Brackx, V. Grosu, H. Cuypers, J. Geeroms, M. Moltedo, B. Vanderborght and D. Lefeber, “Mechatronic Design of a Sit-to-Stance Exoskeleton,” In: *Proceedings of the 5th Biomedical Robotics and Biomechanics (BioRob)* (2014) pp. 945–950.
- [9] K. Kamali, A. A. Akbari and A. Akbarzadeh, “Trajectory generation and control of a knee exoskeleton based on dynamic movement primitives for sit-to-stand assistance,” *Advanced Robotics* **30**(13), 846–860 (2016).
- [10] N. Yangn, “Apparatus for palpitating walking, running, and jumping,” *U.S. Patent*, No. **420**, 179 (1890).
- [11] S. H. Collins, M. B. Wiggin and G. S. Sawicki, “Reducing the energy cost of human walking using an unpowered exoskeleton,” *Nature* **522**(7555), 212–215 (2015).
- [12] P. Cherelle, V. Grosu, A. Mathtys, B. Vanderborght and D. Lefeber, “Design and validation of the ankle mimicking prosthetic (AMP-) foot 2.0,” *IEEE Trans. Neural Syst. Rehab. Eng.* **22**(1), 138–148 (2013).
- [13] H. Hirai, R. Ozawa, S. Goto, H. Fujigaya, S. Yamasaki, Y. Hatanaka and S. Kawamura, “Development of An Ankle-Foot Orthosis with a Pneumatic Passive Element,” In: *Proceedings of the 15th IEEE International Symposium on Robot and Human Interactive Communication* (2006) pp. 220–225.
- [14] C. J. Walsh, K. Endo and H. Herr, “A quasi-passive leg exoskeleton for load-carrying augmentation,” *Int. J. Human. Robot.* **4**(03), 487–506 (2007).
- [15] S. Pardoel and M. Doumit, “Development and testing of a passive ankle exoskeleton,” *Biocybern. Biomed. Eng.* **39**(03), 902–913 (2019).
- [16] W. Van Dijk, H. Van der Kooij and E. Hekman, “A Passive Exoskeleton with Artificial Tendons: Design and Experimental Evaluation,” In: *Proceedings of the IEEE International Conference on Rehabilitation Robotics* (2011) pp. 1–6.
- [17] H. Lee, S. H. Kim and H.-S. Park, “A fully soft and passive assistive device to lower the metabolic cost of sit-to-stand,” *Front. Bioeng. Biotechnol.* **8**, 1–11 (2020).
- [18] F. A. Panizzolo, C. Bolgiani, L. Di Liddo, E. Annesse, and G. Marcolin, “Reducing the energy cost of walking in older adults using a passive hip flexion device,” *J. Neuroeng. Rehab.* **16**(1), 1–9 (2019).
- [19] L. C. Rome, L. Flynn and T. D. Yoo, “Rubber bands reduce the cost of carrying loads,” *Nature* **444**(7122), 1023–1024 (2006).
- [20] F. L. Haufe, P. Wolf, R. Riener and M. Grimmer, “Biomechanical effects of passive hip springs during walking,” *J. Biomech.* **98**(2), 1–9 (2020).
- [21] J.-t. Zhang, *Passive Lower-Limb Exoskeletons for Human Gait Assistance: Development and Evaluation* (Queen University, 2018).
- [22] R. Nasiri, A. Ahmadi and M. N. Ahmadabadi, “Reducing the energy cost of human running using an unpowered exoskeleton,” *IEEE Trans. Neural Syst. Rehab. Eng.* **26**(10), 2026–2032 (2018).
- [23] R. Chaichaowarat, J. Kinugawa and K. Kosuge, “Unpowered knee exoskeleton reduces quadriceps activity during cycling,” *Engineering* **4**(4), 471–478 (2018).
- [24] M. B. Yandell, J. R. Tacca and K. E. Zelik, “Design of a low profile, unpowered ankle exoskeleton that fits under clothes: Overcoming practical barriers to widespread societal adoption,” *IEEE Trans. Neural Syst. Rehab. Eng.* **27**(4), 712–723 (2019).
- [25] J. Leclair, S. Pardoel, A. Helal and M. Doumit, “Development of an unpowered ankle exoskeleton for walking assist,” *Disabil. Rehab. Assis. Technol.* **8**, 1–13 (2018).
- [26] C. Copilusi, M. Ceccarelli and G. Carbone, “Design and numerical characterization of a new leg exoskeleton for motion assistance,” *Robotica* **33**(5), 1147–1162 (2015).
- [27] X. Guan, L. Ji, R. Wang and W. Huang, “Optimization of An Unpowered Energy-Stored Exoskeleton for Patients with Spinal Cord Injury,” In: *Proceedings of the 38th Annual International Conference of the IEEE Engineering in Medicine and Biology Society (EMBC)* (2016) pp. 5030–5033.
- [28] P. Krepelka, I. Hynstova, R. Pytel, F. Prez-Rodriguez, J. M. Roger and P. Drexler, “Curve fitting in Fourier transform near infrared spectroscopy used for the analysis of bacterial cells,” *J. Near Infrared Spectro.* **25**(3), 151–164 (2017).
- [29] F. C. Anderson and M. G. Pandy, “Dynamic optimization of human walking,” *J. Biomech. Eng.* **123**, 381–390 (2001).
- [30] M. K. Starr, “Modular production—a new concept,” *Harvard Bus. Rev.* **43**(6), 131–142 (1965).
- [31] S. Lee, S. Lee, Y. Na, B. Ahn, H. Jung, S. S. Cheng, N. Kim, T.-S. Jun and Y. Kim, “Shock absorber mechanism based on an SMA spring for lightweight exoskeleton applications,” *Int. J. Precis. Eng. Manuf.* **20**(9), 1533–1541 (2019).
- [32] J. Masood, J. Ortiz, J. Fernandez, L. A. Mateos and D. G. Caldwell, “Mechanical Design and Analysis of Light Weight Hip Joint Parallel Elastic Actuator for industrial exoskeleton,” In: *Proceedings of the 6th IEEE International Conference on Biomedical Robotics and Biomechanics (BioRob)* (2016) pp. 631–636.
- [33] C. Di Natali, T. Poliero, M. Sposito, E. Graf, C. Bauer, C. Pauli, E. Bottenberg, A. De Eyto, L. O’Sullivan and A. F. Hidalgo, “Design and evaluation of a soft assistive lower limb exoskeleton,” *Robotica* **37**(12), 2014–2034 (2019).

- [34] B. R. Umberger, K. G. M. Gerritsen and P. E. Martin, “A model of human muscle energy expenditure,” *Comput. Meth. Biomech. Biomed. Eng.* **6**(2), 99–111 (2003).
- [35] S. Faraji, A. R. Wu and A. J. Ijspeert, “A simple model of mechanical effects to estimate metabolic cost of human walking,” *Sci. Rep.* **8**(1), 1–12 (2018).
- [36] G. Tang and C. Wang, “A simple model of mechanical effects to estimate metabolic cost of human walking,” *J. Biomed. Eng.* **27**(5), 987–990 (2010).